Creation of free excitons in solid krypton investigated by time-resolved luminescence spectroscopy

2003 J. Phys.: Condens. Matter 15 2023

(http://iopscience.iop.org/0953-8984/15/12/319)

INSTITUTE OF PHYSICS PUBLISHING JOURNAL OF PHYSICS: CONDENSED MATTER

J. Phys.: Condens. Matter **15** (2003) 2023–2032 PII: S0953-8984(03)54531-3

Creation of free excitons in solid krypton investigated by time-resolved luminescence spectroscopy

Vambola Kisand[1,4], Marco Kirm[2], Evgeni Negodin[2], Elke Sombrowski[3], Barbara Steeg[3], Sebastian Vielhauer[2] and Georg Zimmerer[2]

[1] Institute of Physics, University of Tartu, Riia 142, 51014 Tartu, Estonia
[2] Institut für Experimentalphysik der Universität Hamburg, Luruper Chaussee 149, 22761 Hamburg, Germany
[3] DESY, Notkestrasse 85, 22603 Hamburg, Germany

E-mail: vamps@fi.tartu.ee

Received 9 October 2002
Published 17 March 2003
Online at stacks.iop.org/JPhysCM/15/2023

Abstract

The creation and relaxation of secondary excitons in solid Kr was investigated using energy- and time-resolved luminescence spectroscopy in the vacuum ultraviolet region. The spectrally selected emission of the free exciton (FE) was used as a probe for an investigation of the different exciton creation processes. Delayed FE creation via electron–hole recombination and 'prompt' (in terms of the time-resolution of the experiment) creation of excitons were separated.

The 'prompt' creation of a FE appears in the region above threshold energy E_{th}, which is equal to the sum of the band gap energy and the free exciton energy. 'Prompt' creation of excitons above E_{th} is ascribed to a superposition of two processes: (i) creation of the electronic polaron complex (one-step process) and (ii) inelastic scattering of photoelectrons described in the framework of the multiple-parabolic-branch band model (two-step process).

In addition, the ratio spectrum of the time-integrated FE and self-trapped exciton (STE) emission was analysed. The behaviour of the ratio spectrum is a proof that electron–hole recombination leads to STE states through FE states as precursors.

1. Introduction

Solid Kr is an ideal model substance for investigations of excitonic excitations in insulators. Excitonic effects are observable both in absorption/reflection and in the emission spectra of solid Kr [1–3]. The most interesting aspect of excitonic luminescence in solid Kr is the coexistence of free excitons (FEs) and self-trapped excitons (STEs) due to the energy barrier

[4] Author to whom any correspondence should be addressed.

0953-8984/03/122023+10$30.00

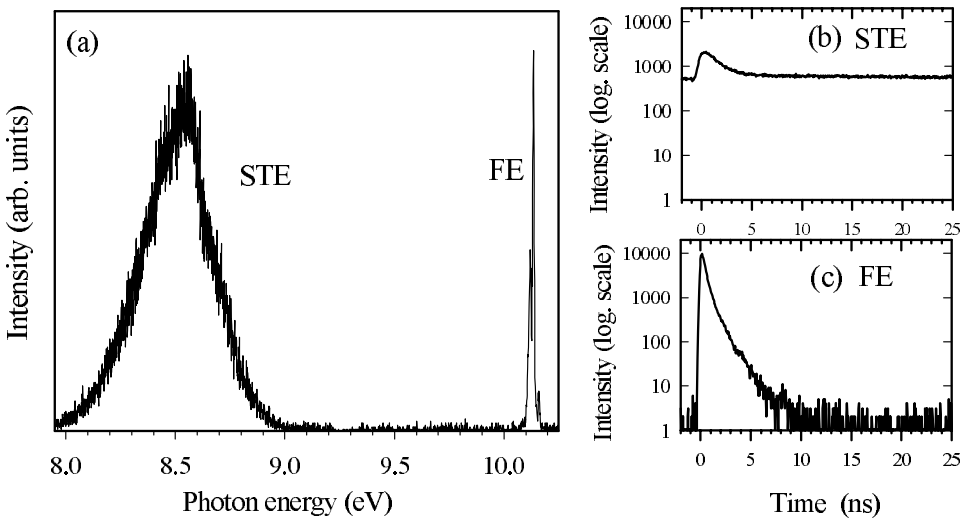

Figure 1. (a) Typical emission spectrum of a good quality Xe-free Kr sample excited by 10.42 eV photons at 6 K. Resolution of the analysing monochromator was $\Delta\lambda = 1.2$ Å. (b) The decay curve of STE emission in solid Kr. (c) The decay curve of FE emission in solid Kr. Both decay curves are excited by 10.42 eV photons at 6 K. STE emission was measured at 8.55 eV and FE luminescence at 10.14 eV (analysing monochromator resolution $\Delta\lambda = 9$ Å).

separating the respective states. As a result, strong broad-band STE emission (maximum at ∼8.6 eV) as well as pronounced narrow-band emission of FEs ($E_{ex} = 10.14$ eV) are simultaneously observable.

In the present work, good quality solid krypton samples were grown, since significant FE emission is observable only in this type of sample. The influence of the sample quality on the emission spectrum of solid krypton was discussed in detail in our previous paper [4]. By good quality samples we mean such polycrystalline samples where the size of the microcrystallites is significantly larger than the scattering length of a FE on acoustic phonons. Practically Xe-free Kr gas was used for sample preparation, because even some tens of ppm Xe in Kr cause strong Xe emission, suppressing the FE luminescence of solid Kr. A typical emission spectrum of a good quality Xe-free Kr sample is shown in figure 1(a).

The main subject of the present work is the investigation of the different exciton creation processes using tunable photoexcitation, where the photon energy exceeds the band gap energy. Previous studies of the FE luminescence of solid Kr were mainly restricted to the excitonic energy region [3, 5, 6]. Due to their simple crystalline structure (monoatomic fcc lattice) optical phonons are absent in rare gas crystals (RGC). All phonon-assisted relaxation processes are therefore slowed down in comparison to alkali halide crystals. Because of this unique property it is possible to distinguish between different relaxation processes in solid krypton on a nanosecond timescale.

Though the STE luminescence signal is much stronger, the FE emission of solid krypton was used as a probe for the following reasons. STE luminescence is a superposition of emissions arising from two different states of the STE: the singlet and the triplet state. The decay of the singlet component is detectable in the nanosecond range, but the strong triplet component with a microsecond decay gives rise to a strong background, masking effects observable only in the first few nanoseconds. In figure 1 the decay curves of FE (b) and STE (c) luminescence, excited in the $n = 1$ exciton peak, are shown for comparison. Additionally,

the self-trapping process is an extra relaxation step, which complicates the analysis. Therefore, FE luminescence is better suited as a probe of exciton creation processes.

2. Experimental details

The experiments were carried out at the experimental station SUPERLUMI located in HASYLAB (*Hamburger Synchrotronstrahlungslabor*) at DESY (*Deutsches Elektronen-Synchrotron*) [7]. Selective photon excitation with a typical resolution of $\Delta\lambda = 3.2$ Å was used. Spectral- and time-resolved analysis of luminescence was carried out with a high-flux VUV monochromator (typical resolution $\Delta\lambda = 8$ Å) and a microsphere plate detector. At HASYLAB, the synchrotron radiation pulses have a FWHM of 130 ps. Due to the response of the detector and the electronics used, the measured FWHM of the excitation pulse was 350 ps. Reflection spectra were recorded simultaneously with excitation spectra at the angle of incidence 17.5°. The time-integrated emission spectrum in figure 1(a) was measured using a high-resolution VUV monochromator in combination with a multichannel plate type position sensitive detector (resolution $\Delta\lambda = 1.2$ Å).

The crucial part of the experiments was sample preparation. Good quality polycrystalline Kr samples with a thickness of about 0.3 mm were grown from the gas phase (with an average growing rate of 2 μm min^{-1}) near thermodynamic equilibrium conditions at 84 K. Finally, the crystals were slowly cooled down (about 1 K min^{-1}). For sample preparation, krypton with the highest commercially available purity (Spectra Gases Inc., 99.999%, Xe less than 5.0 ppm) was used. During measurements, the pressure in the sample chamber was below 1×10^{-9} mbar.

3. Decay of free excitons

FE decay curves excited with different photon energies are presented in figure 2. The time structure of the exciting light pulse is shown at the bottom of the figure. In the time structure of the synchrotron radiation, side bunches with 2 ns periodicity following the main bunch are detected during the beam time period used. Since the maximal relative intensity of the side bunches was less than 0.005 compared to the main bunch ($t = 0$ ns), their influence on the shape of decay curves is negligible.

As figure 2 demonstrates, the variation of photon energy of excitation causes considerable changes in the shape of FE decay curves. Namely, different processes of FE creation are responsible for the characteristic shapes of the FE decay curves. In the energy range of SUPERLUMI, three regions with different FE creation processes are separable on the basis of the decay curves and excitation spectra:

(i) $E_{ex} < h\nu < E_g$. In the case of photoexcitation energies between the FE energy E_{ex} ($E_{ex} = 10.14$ eV) and band gap energy E_g ($E_g = 11.59$ eV), direct optical creation of excitons occurs. After their creation, excitons relax very quickly (in comparison with the time resolution of experiment) to the lowest FE state. Radiative decay and self-trapping depopulate this FE state. As shown in figure 2 the decay curves in the case of excitonic excitation show a non-exponential behaviour. Such temporal behaviour of the FE luminescence in solid Xe and Kr was analysed in a three-step model by Varding *et al* [6, 8].

(ii) $E_g < h\nu < E_{th}$. Using primary excitation energies exceeding the forbidden gap energy ($h\nu > E_g$), i.e. creating free electron–hole pairs, the situation becomes more complicated. The FE decay exhibits a 'prompt' component (the maximum conforms with the excitation

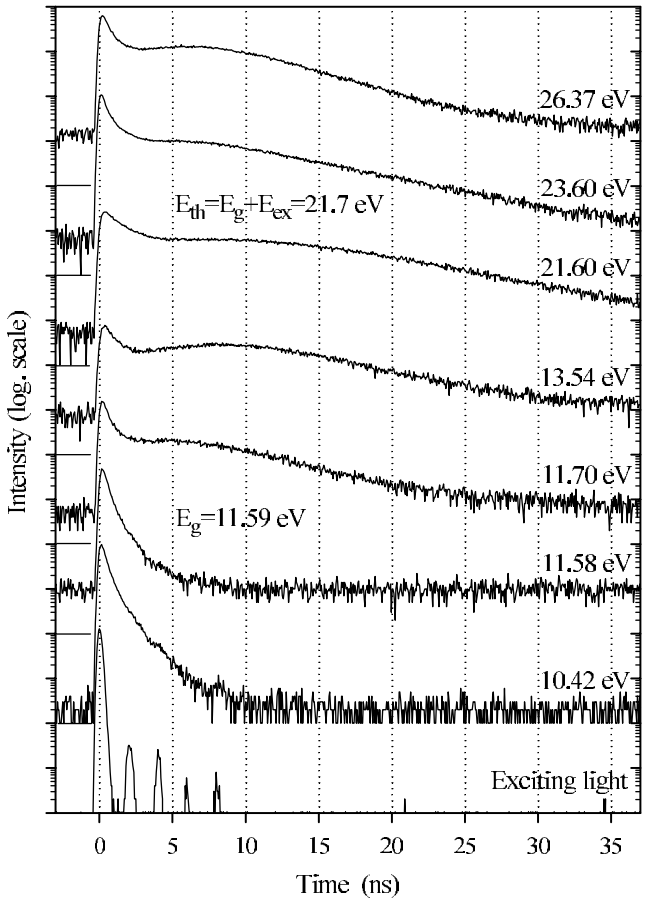

Figure 2. Decay curves of FE luminescence in solid Kr for a typical good quality sample at 5 K. The shape of the excitation pulse is shown at the bottom. Time $t = 0$ corresponds to the maximum signal intensity of the excitation pulse. Excitation energies are shown in the figure above the respective curves. The resolution of the analysing monochromator was set to $\Delta\lambda = 8$ Å.

pulse) and a 'slow' component with a clearly distinct additional delayed maximum (see figure 2). The 'prompt' part is superimposed on the rising part of the 'slow' component. Figure 2 shows clearly that the 'slow' component exists only when exciting above the forbidden gap. It means that the 'slow' component is caused by FE creation through electron–hole recombination. More precisely, the 'slow' component is a convolution of the temporal evolution of electron–hole recombination into an excitonic state and the decay of the free excitons. It is quite natural that by increasing the excitation energy, electrons with higher kinetic energy need more time to relax down to the bottom of the conduction band and the maximum of the 'slow' component becomes more delayed. A similar behaviour of FE luminescence following creation of free electron–hole pairs is also observed for solid Xe [9]. The decay curves of FE emission in solid Xe were reproduced with model calculations [9]. The model used for FE formation via electron–hole recombination includes (i) creation of electron–hole pairs in photoexcitation, (ii) thermalization of carriers via scattering on acoustic phonons, and (iii) carrier recombination into the FE state.

In our recent paper [10] we demonstrated that applying a similar model it is also possible to simulate experimental decay curves of the 'slow' component for solid Kr. However, the

use of this model is restricted to the excitation region $E_g < h\nu \lesssim E_g + 1.5$ eV. Namely, the parabolic band approximation of the model is only valid for a limited energy range.
For solid Kr, it is generally supposed that holes self-trap within a few picoseconds. This means that recombination of mobile electrons and self-trapped holes leads to the formation of a delocalized FE. This is far from non-trivial because in the past it was assumed that trapped holes capture electrons forming STEs. The latter mechanism is not ruled out by the results of our work, but this is at least not the only recombination process. Whether the STE formed after the creation of free electron–hole pairs originates exclusively either from self-trapping of free excitons or from the capture of electrons by self-trapped holes will be discussed in section 5 of this paper.
The nature of the 'prompt' component in this energy region is not well understood. Partly, it can be an experimental artefact originating from the FE luminescence signal excited by scattered light of the primary monochromator. On the other hand, it cannot be excluded that the 'prompt' component has an unknown physical origin. Consequently, the origin of the 'prompt' component needs additional investigation.

(iii) $h\nu > E_{th}$. The shape of the decay curves changes significantly above a threshold energy $E_{th} \approx 21.7$ eV. The energy value of this threshold is deduced from the time-resolved excitation spectra (see next section). This threshold value is nearly equal to the sum of the band gap energy and the free exciton energy ($E_{th} \approx E_g + E_{ex}$). As figure 2 shows, the intensity of the 'prompt' part of the FE decay curves increases essentially above this threshold. This effect is caused by the prompt creation of two excitations per absorbed photon, which becomes possible above the threshold at $E_{th} \approx 21.7$ eV. The origin of this threshold will be discussed in more detail in the next section.

4. Time-resolved excitation spectra of FE luminescence

While measuring time-resolved excitation spectra, two time-related parameters can be varied: the length of the time window (Δt) and the delay of the time window due to the excitation pulse (δt; in this work, it is calculated starting from the *maximum* of the exciting light peak). Time-resolved excitation spectra of FE luminescence are presented in figure 3. The time windows are: 'hot' ($\Delta t = 0.94$ ns, $\delta t = 0$ ns), 'short' ($\Delta t = 1.57$ ns, $\delta t = 0.59$ ns), 'long' ($\Delta t = 5.04$ ns, $\delta t = 2.57$ ns) and 'very long' ($\Delta t = 32.5$ ns, $\delta t = 7.2$ ns). This 'notation' of the time windows will be used in the following discussions. For comparison, the time-integrated FE excitation spectrum and the reflection spectrum are also shown. The latter one indicates changes in the absorption coefficient of a Kr crystal.

Depending on the delay time and the length of the time window, different relaxation processes are observed. It is important to note that the 'prompt' processes (in terms of the time resolution of the experiment) are observable not only in the 'hot' time window but the 'prompt' processes also contribute to some extent to the time windows with longer delay, because the decay of the 'prompt' excitons extends even to longer times.

Immediate creation of a FE ('hot' window, $\Delta t = 0.94$ and $\delta t = 0$ ns) is predominant in two regions: in the excitonic region ($h\nu < E_g$) and in the region above the experimental threshold ($h\nu > E_{th} \approx 21.7$ eV). In the excitonic region, direct creation of excitons and their fast phonon-assisted relaxation to the lowest FE state occurs.

The value of the experimental threshold $E_{th} \approx 21.7$ eV was determined with an accuracy of ± 0.2 eV from excitation spectra measured in a 'hot' time window. The measurements were performed for several samples. The threshold is always distinct and reproducible. However, some differences were observed in the shape of the spectra above the threshold for different samples.

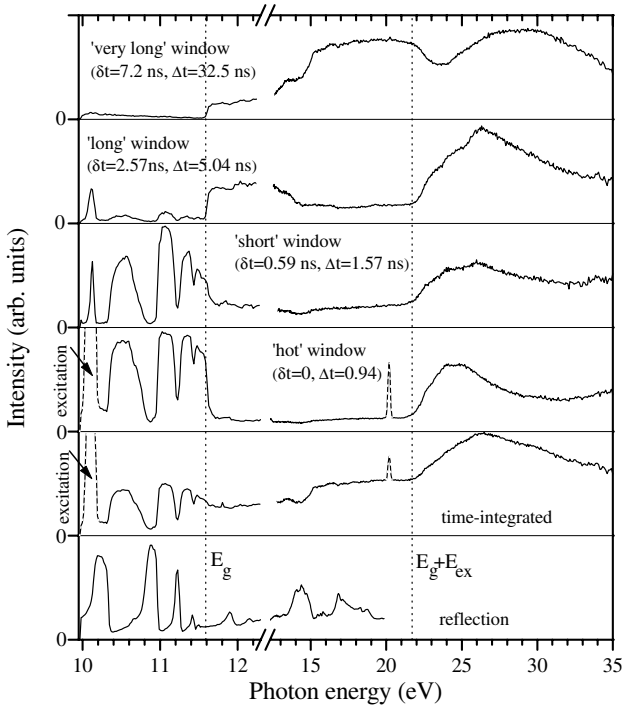

Figure 3. Time-integrated and time-resolved excitation spectra of FE luminescence for a typical good quality sample at 10.1 eV ($T = 6$ K). The resolution of the primary monochromator was 2.2 Å (in excitation) and of the analysing monochromator was set to 11 Å (in emission). For comparison, the reflection spectrum is also shown. The sharp peaks slightly above 20 eV, pronounced in the 'hot' time window and time-integrated spectra, are caused by the second order of the analysing monochromator. The parameters of the time windows are denoted in the figure.

The threshold at $E_{th} \approx 21.7$ eV can be explained (i) by secondary exciton creation via inelastic scattering of 'hot' photoelectrons in a two step process [11], or (ii) by simultaneous creation of a FE and an electron–hole pair in a one-step process (electronic polaron complex) [12]. The theoretical threshold for creation of an electronic polaron complex is predicted at $E_{th} = E_g + E_{ex}$ [12].

The simplest 'classical' single-parabolic-branch band (SPBB) model of electron–electron scattering takes into account transitions only within one parabolic band in k-space [13], while the more complicated multiple-parabolic-branch band (MPPB) model of electron–electron scattering includes transitions between the different branches [11]. The equations for threshold energies for creation of two excitations using the SPBB model are given in [13] and using the MPBB model in [11]. It turns out that the theoretical threshold energy for the creation of an exciton and an electron–hole pair using the simplest SPBB model is always significantly larger than $E_g + E_{ex}$ because part of the absorbed photon energy is divided between the created electron and hole reciprocally to their effective masses. In the MPBB model, it has been shown that the smallest theoretical threshold energy for FE and electron–hole pair creation in the electron–electron scattering process is $E_{th} \approx E_g + E_{ex}$. Consequently, it is possible to explain the experimental threshold $E_{th} \approx 21.7 \pm 0.2$ eV using the MPBB model describing electron–electron scattering as well [11]. However, the MPBB model also considers the conduction band using the parabolic approximation, neglecting the real electronic structure

of the conduction band. In addition, it is important to note that in solid Kr the width of the valence band (2.3 eV [14]) is much smaller than the band gap energy ($E_g = 11.59$ eV) and therefore 'hot' holes cannot create any secondary electronic excitations.

The formation of two electronic excitations per one absorbed photon also has an influence on the distribution of emitted photoelectrons. Below the threshold, photoelectrons with high kinetic energy ($\sim$10 eV) are observed. Above the threshold, an exciton and an electron–hole pair with low kinetic energy are created, leading to the enhanced emission of low energy electrons. According to the photoemission data of [14, 15] a sudden increase in the number of low energy photoelectrons takes place above 21.6 eV, being in good agreement with our value E_{th}.

Accordingly the two different models (MPBB model of electron–electron scattering, creation of an electronic polaron complex) predict the same theoretical threshold at $E_{th} = E_g + E_{ex} \approx 21.7$ eV which is in very good agreement with the experimental value $E_{th} \approx 21.7 \pm 0.2$ eV. A remarkable change in the shape of the FE decay curves also correlates with this threshold (see figure 2). However, it is not possible to discriminate between the two models using only photoexcitation experimental data. Independently of the origin of the threshold, it is reasonable to assume that the structures above the threshold in the 'hot' time window include both processes, the FE creation via electron–electron scattering and the creation of an electronic polaron complex.

Although the threshold itself is due to the creation of an exciton and an electron–hole pair, at higher photon energies the creation of two electron–hole pairs occurs as well. The uppermost curve in figure 2 excited by 26.37 eV photons again resembles the curves obtained at photon energies above E_g, and the electrons with small kinetic energy are again close to the bottom of the conduction band shifting the maximum of the 'slow' component back to shorter times. However, the shape of the 'slow' component above E_{th} is not so well defined compared to that directly excited above E_g, since the energy available can be distributed differently between the two electrons in the conduction band at a given exciting photon energy.

A similar threshold at $E_{th} = E_g + E_{ex}$ was also observed in solid xenon [16, 17]. In solid xenon, Steeg *et al* observed a double peak structure above the threshold, most probably caused by the spin–orbit splitting of the valence band. The splitting of the maximum above E_{th} is not clearly identified for solid Kr. Nevertheless, a small plateau on top of the maximum (from 24 to 25 eV in the 'hot' time window) is visible. In solid Xe, the spin–orbit splitting is significantly larger (1.37 eV) than in solid Kr (0.70 eV) [18]. Therefore, the origin of the plateau from 24 to 25 eV in the 'hot' window of solid krypton is also tentatively ascribed to spin–orbit splitting.

The contribution of slow electron–hole recombination increases in the time windows with a longer delay δt. After a sufficiently long delay all other possible creation mechanisms of FEs, except the electron–hole recombination, are excluded. The meaning of 'sufficiently long' is not well defined, being primarily determined by the decay time of the FE. In figure 3, a 'very long' time window with a delay $\delta t = 7.2$ ns is shown. The intensity of the 'prompt' component is practically diminished to the detector noise level after such a delay (see figure 2).

In the 'very long' time window ($\delta t = 7.2$ ns), the FE creation through electron–hole recombination starts at the forbidden gap energy (a well pronounced step at 11.6 eV in figure 3). In the energy range $E_g < h\nu < E_{th}$, the intensity in the 'very long' time window rises as well. This is due to the retardation of electron–hole recombination, which shifts the intensity maximum of the 'slow' component of FE decay curves to longer times, i.e. more intensity is detected within this time window. The intensity modulations of excitation spectra in this energy range can be explained by variation of the absorption coefficient (compare with the reflection spectrum in figure 3).

Above the threshold E_{th}, the creation of two electronic excitations takes place introducing changes in the excitation spectra. The intensity increase takes place in all time windows, except the 'very long' time window. The decrease in the intensity within the 'very long' time window above E_{th} does not imply a reduction in the number of created electron–hole pairs, but is rather the effect of a smaller kinetic energy of the created electrons. The number of created electron–hole pairs slightly above E_{th} is the same as below E_{th}, since the photon energy is sufficient to create an electron–hole pair plus an exciton, but not yet two electron–hole pairs. An intensity growth in the 'very long' time window at $\sim$ 24 eV is caused by the following:

(i) photons have now sufficient energy for creation of two electron–hole pairs,
(ii) the initial kinetic energy of the electrons in the conduction band also increases and the maximum of the 'slow' component of the decay curve shifts again to longer times, i.e. the number of emitted photons in the 'very long' time window increases.

The spectra measured in two intermediate time windows ('short' and 'long') in figure 3 reflect the 'prompt' FE creation processes as well as the 'slow' FE creation through electron–hole recombination. The 'prompt' FE creation dominates in the 'short' time window ($\delta t = 0.59$ ns) and the electron–hole recombination in the 'long' time window ($\delta t = 2.57$ ns).

In the past, Biester *et al* investigated photoemission of pairs of electrons [19] (coincidence measurements). Secondary double photoemission is a process where the absorption of a photon by one atom is followed by the ejection of an electron with kinetic energy high enough to ionize a second atom by electron–electron scattering. Such a process has been detected with surprisingly high efficiency in solid Kr excited by photons above 25 eV [19]. Hence, such phenomena should also be indirectly observable in our experiment as well. The double photoemission results in the production of two low energy electrons with non-discrete energy distribution. Its possible manifestations are expected in the 'very long' time window, where recombination of slow electrons with holes contributes to the formation of free excitons. The threshold observed by Biester includes twice the energy of the vacuum level (2*0.3 eV [14]). In the present case, a value around 24.4 eV is expected. This corresponds quite well to the increase in the signal in the 'very long' time window at $\sim$24 eV.

Finally, we point out that such an amount of information about formation of secondary excitons and electron–hole pairs can be acquired only from time-resolved excitation spectra. The smooth time-integrated excitation spectrum of FE emission with fewer features shown in figure 3 demonstrates that the contribution of various processes mask each other.

5. Ratio of FE and STE luminescence excitation spectra

The ratio of the time-integrated FE and STE excitation spectra (ratio spectrum) offers additional information about creation and relaxation of electronic excitations. At the same time, all kinds of possible FE and STE creation processes contribute to the ratio spectrum and therefore an interpretation of such a spectrum is far from non-trivial. Figure 4 depicts the FE/STE ratio spectrum for a typical good quality sample of solid Kr. For comparison, the reflection spectrum for the same sample is also shown. The sharp narrow minimum at $\sim$17 eV and maximum at $\sim$20 eV are caused by the second order of the analysing monochromator. The ratio spectra exclude experimental inaccuracies caused by the normalization of the recorded spectra. Moreover, the disturbing influence of the reflection coefficient is removed, since reflection losses are included in both excitation spectra, cancelling each other out in the ratio spectra.

In the excitonic region, the modulations in the ratio spectra demonstrate that FE creation is more probable (or STE creation is less probable), if the penetration depth of the exciting light is

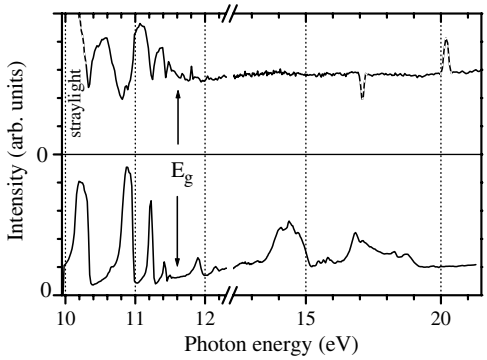

Figure 4. Ratio spectrum of the time-integrated FE and STE emissions as a function of photon energy of excitation for a typical good quality sample. FE emission was measured at 10.1 eV and STE emission at 8.55 eV. The sharp dashed minimum at ∼17 and maximum at ∼20 eV are caused by the second order of the analysing monochromator. The reflection spectrum for the same sample is also shown at the bottom. The resolution of the primary monochromator was 2.2 Å (in excitation) and the resolution of the analysing monochromator was set to 11 Å (in emission).

larger (i.e. the absorption coefficient is smaller). The correlations of modulations in this range with the penetration depth of the exciting light might be caused by variations of the balance between radiative FE decay and self-trapping. It is entirely reasonable that self-trapping is more favourable near the surface than in the bulk.

In the region above the band gap energy ($E_g < h\nu$), the creation of the STE is clearly proportional to the creation of the FE. The smooth behaviour of the FE/STE ratio spectra above the band gap is a definite proof that the STE originating from electron–hole recombination has FE states as precursors. In other words, recombination leads to the creation of free excitons which then either radiate or get localized into the STE state. The FE/STE ratio spectrum was also analysed for solid Xe [16] and this spectrum demonstrated a similar behaviour.

6. Conclusions

In the present work, time-resolved excitation spectra of FE emission in solid Kr were measured for the first time, using VUV excitation up to ∼35 eV. Moreover, FE luminescence decay curves were systematically investigated in the same energy range. Such measurements were possible due to the intense FE emission, connected with the very good quality of the samples grown from Kr gas of very high purity. A series of samples was grown and investigated, demonstrating a good reproducibility of the main experimental results.

Delayed creation of excitons via electron–hole recombination and 'prompt' (in the meaning of the time resolution of experimental set-up) creation of excitons were clearly separated using the time-resolved experimental technique. If the exciting photon energy is smaller than the band gap, $h\nu < E_g$ ($E_g = 11.59$ eV), direct optical creation of excitons occurs. After their creation, excitons relax 'promptly' to the lowest FE state and then emit FE luminescence or become self-trapped. Using primary excitation energy exceeding the forbidden gap energy ($h\nu > E_g$), i.e. creating electron–hole pairs, the FE decay curve exhibits the 'prompt' component (the maximum is conforming with the excitation pulse) and also a 'slow' component with an additional delayed maximum.

It was experimentally demonstrated that preferential prompt creation of FE not only takes place in the excitonic region, but also above the threshold $E_{th} \approx 21.7$ eV. The experimental

threshold value is nearly equal to the sum of the band gap energy and the free exciton energy ($E_{th} = E_g + E_{ex}$). 'Prompt' creation of excitons above E_{th} is ascribed to a superposition of two processes:

(i) inelastic scattering of the electrons in the framework of the MPPB model (two-step process), and
(ii) creation of the electronic polaron complex (one-step process).

At the threshold itself, the creation of the electronic polaron complex may be the dominant process, and at higher excitation energies, electron–electron scattering prevails.

Additionally the ratio spectrum of the time-integrated FE and STE emissions of solid Kr was analysed for the first time. The smooth behaviour of the FE/STE ratio spectrum above the band gap shows that the STE originating from electron–hole recombination has FE states as precursors. In other words, recombination leads to the creation of free excitons which then either decay radiatively or get localized into the STE state.

Acknowledgments

This work was supported by the Deutsche Forschungsgemeinschaft (project DFG-Zi 159/2) and Bundesministerium für Bildung und Forschung (grant 05 ST8GUI 6). VK also gratefully acknowledges support of the EC FW5 'Centres of Excellence' programme (project ICA1-1999-70086) and the Estonian Science Foundation (grant 4508).

References

[1] Baldini G 1962 *Phys. Rev.* **128** 1562
[2] Zimmerer G 1987 *Excited State Spectroscopy in Solids* ed U M Grassano and N Terzi (Amsterdam: North-Holland) p 37
[3] Varding D, Becker J, Frankenstein L, Peters B, Runne M, Schröder A and Zimmerer G 1993 *Low Temp. Phys.* **19** 427
[4] Kisand V, Kirm M, Vielhauer S and Zimmerer G 2002 *J. Phys.: Condens. Matter* **14** 5529
[5] Kloiber T 1989 *PhD Thesis* The University of Hamburg
[6] Varding D 1994 *PhD Thesis* The University of Hamburg
[7] Zimmerer G 1991 *Nucl. Instrum. Methods Phys. Res.* A **308** 178
[8] Varding D, Reimand I and Zimmerer G 1994 *Phys. Status Solidi* b **185** 301
[9] Reimand I, Gminder E, Kirm M, Kisand V, Steeg B, Varding D and Zimmerer G 1999 *Phys. Status Solidi* b **214** 81
[10] Kisand V, Kirm M, Vielhauer S and Zimmerer G 2002 *Surf. Rev. Lett.* **9** 783
[11] Vasil'ev A N, Fang Y and Mikhailin V V 1999 *Phys. Rev.* B **60** 5340
[12] Devreese J T, Kunz A B and Collins T C 1972 *Solid State Commun.* **11** 673
[13] Lushchik A, Feldbach E, Kink R, Lushchik C, Kirm M and Martinson I 1996 *Phys. Rev.* B **53** 5379
[14] Schwentner N, Himpsel F J, Saile V, Skibowski M, Steinmann W and Koch E E 1975 *Phys. Rev. Lett.* **34** 528
[15] Schwentner N 1976 *Phys. Rev.* B **14** 5490
[16] Steeg B 1999 *PhD Thesis* The University of Hamburg
[17] Steeg B, Gminder E, Kirm M, Kisand V, Vielhauer S and Zimmerer G 1999 *J. Electron Spectrosc. Relat. Phenom.* **101** 879
[18] Rössler U 1970 *Phys. Status Solidi* **42** 345
[19] Biester H W, Besnard M J, Dujardin G, Hellner L and Koch E E 1987 *Phys. Rev. Lett.* **59** 1277